Available online at www.sciencedirect.com
ScienceDirect
Ceramics International 36 (2010) 2273–2280
CERAMICS INTERNATIONAL
www.elsevier.com/locate/ceramint

Phase evolution and thermophysical properties of plasma sprayed thick zirconia coatings after annealing

Giovanni Di Girolamo [a,b,*], Caterina Blasi [a], Leonardo Pagnotta [b], Monica Schioppa [a]

[a] ENEA, UTTMATB, Brindisi Research Centre, S.S. 7 Appia, km 713.7, 72100 Brindisi, Italy
[b] Department of Mechanical Engineering, University of Calabria, Ponte Pietro Bucci Cubo 44C, 87036 Rende (CS), Italy

Received 2 April 2010; received in revised form 5 April 2010; accepted 30 May 2010
Available online 3 August 2010

Abstract

Yttria partially stabilized zirconia (YSZ) thick thermal barrier coatings were fabricated by Atmospheric Plasma Spraying (APS) and isothermally annealed at 1315 °C for different durations. The phase composition of as-sprayed and heat-treated free-standing coatings was investigated by X-ray Diffraction (XRD) and the Rietveld method was employed for quantitative phase analysis. High-temperature exposure of YSZ coatings produced the partial decomposition of metastable t' zirconia phase and the corresponding increase in the amount of stable tetragonal t, cubic c and monoclinic m phases with increasing the aging time.

The thermophysical properties of as-sprayed and annealed YSZ coatings, such as thermal expansion and heat capacity, were measured. The thermal expansion coefficient kept almost constant in-plane direction after heat treatment. Otherwise, it changed in through-thickness direction due to any structural changes and high-temperature sintering of the porous microstructure. The sintering also influenced the specific heat capacity C_p which increased with increasing the annealing time.

Keywords: A. Plasma spraying; C. Thermal properties; D. ZrO2; E. Thermal applications

1. Introduction

Ceramic thermal barrier coatings (TBCs) are advanced engineered systems which are currently adopted to thermally insulate the surface of metal components from severe operating environments typical of gas turbine and diesel engines, in order to extend their lifetime at in-service conditions. In addition, TBCs are powerful tools to enhance engine efficiency and performance, in terms of higher operating temperatures or lower cooling air flow, as well as lower emissions and lower fuel consumption.

Plasma spraying is a cost-effective technology for manufacturing of porous TBCs. Powder particles are injected into a high-temperature plasma gas jet, melted and accelerated. When they impact on the substrate, are flattened and quenched, thus forming a coating with layered microstructure containing globular pores and microcracks [1].

Thick TBCs (~1–2 mm) are particularly suitable to protect combustion chamber components, where the failure mechanism is mainly affected by hot corrosion, thermal cycling and mechanical loads [2]. A thick coating typically provides a higher temperature drop through the thickness and, at the same time, increases the elastic strain energy stored and the energy release rate for crack formation and propagation. Indeed, higher stresses are expected during service, due to the thermal expansion mismatch between the ceramic coating and the metal substrate [3].

To this purpose, Vassen et al. have reported thermal expansion coefficients (CTEs) of $16 \times 10^{-6}\,K^{-1}$ for IN738 superalloy substrates and of $17.5 \times 10^{-6}\,K^{-1}$ for a typical CoNiCrAlY coating, in the temperature range between 20 and 1000 °C [4]. Therefore, the fabrication of ceramic coatings with large thermal expansion coefficient ($>10 \times 10^{-6}\,K^{-1}$), optimized porosity volume (10% or higher) and good strain tolerance, *i.e.* low Young's modulus, represents an essential key factor [1].

Yttria partially stabilized zirconia (YSZ) represents the current state-of-the-art material used in industrial applications, because it provides a good compromise between the basic requirements demanded to TBC materials, such as low thermal

* Corresponding author at: UTTMATB, ENEA, Brindisi Research Centre, S.S. 7 Appia, km 713.7, 72100 Brindisi, Italy. Fax: +39 0831 201581.
E-mail address: giovanni.digirolamo@enea.it (G. Di Girolamo).

0272-8842/$36.00
doi:10.1016/j.ceramint.2010.07.035

conductivity (2.1–2.2 W m^{-1} K^{-1} for bulk zirconia), good phase stability, thermal expansion coefficient (CTE) close to that of metal substrate, low sintering rate and good strain tolerance. The researches about new materials with low thermal conductivity have been notably increased in the last years [5–9]. However, further studies about the stability of plasma sprayed YSZ coatings properties at high temperature are needed and thus the literature about this material is implementing by new contributions [8,10,11]. In particular, the knowledge of the structural and thermophysical properties of YSZ coatings exposed at high temperature is fundamental to predict their performance during long-term service.

To this purpose, phase stability of heat-treated YSZ coatings has been studied in many previous works [12–16]. However, there are some mismatches between the results and the mechanism which governs the phase transition, which could be explained in terms of different powder feedstock morphology and grain size, spraying parameters and different cooling rates employed during coating fabrication or high-temperature exposure. As well-known, zirconia may exist in three crystallographic phases, called cubic, tetragonal and monoclinic. It is generally accepted that as-sprayed YSZ coatings are mainly composed of metastable t' zirconia with smaller amounts of cubic and monoclinic phases [11,17]. During cooling to room temperature the tetragonal phase may transform to monoclinic. This transition is accompanied by a volume expansion which can induce significant stresses and, possibly, the nucleation and the propagation of cracks within the TBC, thus reducing its lifetime [18]. In addition, high-temperature sintering can strongly affect the performance of a TBC by a partial reduction of porosity volume and strain tolerance.

In the present work, the effects of high-temperature exposure on the structural and thermophysical properties of YSZ coatings were investigated. To this purpose, high-temperature evolution of thermal expansion and specific heat capacity of YSZ coatings was studied, since CTE plays a significant role on TBC delamination, whereas heat capacity strongly influences the thermal conductivity and the heat transfer to the metal component through coating thickness.

2. Experimental procedure

2.1. Plasma ppraying

YSZ coatings with thickness of about 2 mm were deposited on stainless steel substrates (25 mm × 25 mm × 4 mm) by using an Atmospheric Plasma Spray (Sulzer Metco, Wolhen, Switzerland) equipped with F4-MB plasma torch with 6 mm internal diameter nozzle. To this purpose, the commercial ZrO_2–8 wt.%Y_2O_3 feedstock (Metco 204NS, Sulzer Metco, Westbury, NY) was employed, since the attention of turbine manufacturers is currently focused on this standard composition. The powder contains some impurities, as given by the supplier (see Table 1). YSZ particles have HOSP (homogeneous oven spherical powder) morphology with size ranging from 11 to 125 μm. Spherical hollow particles typically guarantee good flowability and good deposition efficiency. Indeed, they experience a more uniform melting when injected in the plasma plume and are particularly suitable to fabricate porous thermal barrier coatings, due to their lower density with respect to similar particles produced by other manufacturing methods. To this purpose, spray dried and fused and crushed powders can be also used as starting materials in thermal spraying. An intermediate 160 μm thick bond coat was previously deposited by using a commercial feedstock with 38Co–32Ni–21Cr–8Al–0.5Y chemical composition (Amdry 995C, Sulzer Metco, Westbury, NY). Before spraying, the substrates were grit-blasted with alumina abrasive powder (Metcolite F, Sulzer Metco, Westbury, NY) and ultrasonically cleaned in ethanol. Then, they were placed on a rotating sample holder and coated. The plasma spraying parameters used in this work for both bond coat and top coat are summarized in Table 2. In particular, the plasma spraying parameters used for YSZ have been set by using an empirical method based on previous experiments, in the purpose to guarantee a powder feed rate of about 40–50 g/min and a thickness of about 12–15 μm per torch pass. YSZ coatings were produced at high and low substrate temperature, respectively, to study the effect of the cooling rate on the phase composition and the evolution of zirconia phases during re-heating. Two air jets attached to the plasma gun were used for forced air cooling. In this case, the tangential speed was three times higher than that used for slowly cooled coatings (300 and 100 rad/s, respectively).

Table 1
Chemical composition of YSZ powder feedstock (wt.%).

$ZrO_2 + HfO_2$	92.03
Y_2O_3	7.60
HfO_2	1.55
TaO	0.15
TiO_2	0.09
SiO_2	0.07
MgO	0.02
Fe_2O_3	0.01
Al_2O_3	<0.01
CaO	<0.01

Table 2
Plasma spraying parameters used in this work for bond coat and top coat.

Parameter	CoNiCrAlY	YSZ
Current [A]	600	600
Voltage [V]	71.4	64.3
Turntable velocity [rad/s]	50	100
Substrate tangential speed [mm/s]	1041	2083
Gun velocity [mm/s]	4	4
Primary gas Ar flow rate [slpm][a]	55	33
Secondary gas H_2 flow rate [slpm][a]	11	10
Stand-off distance [mm]	120	100
Carrier gas Ar flow rate [slmp][a]	3	2.6
Powder feed rate [g/min]	49.7	42.6
Injector diameter [mm]	1.8	1.8
Injector angle [°]	90	90
Distance torch-injector [mm]	6	6

[a] slpm: standard litres per minute.

The deposition efficiency was calculated from the ratio between the coating mass and the total feedstock mass delivered to the torch, which was determined from the powder feed rate and the spraying time on the substrate. The average deposition rate for YSZ, *i.e.* the thickness per torch pass, was measured by a digital micrometer with a resolution of 1 μm. For slowly cooled coatings, produced at 100 rad/s tangential speed, it was equal to 14.4 μm with a standard deviation of 0.2 μm. In turn, the average deposition efficiency was equal to 53.5%, with a standard deviation of 0.8%. At constant coatings thickness, with increasing the substrate tangential speed up to 300 rad/s, the deposition rate decreased to 12.7 μm (standard deviation = 0.1 μm), while the deposition efficiency decreased to 47.1% (standard deviation = 0.4%).

Before heat treatment, the coatings were cut and stripped off from their substrates by chemical etching, by using a 50/50 (vol.%) HCl–H_2O solution. The acid attacked the interface between bond coat and top coat. Then, the detached ceramic coatings were cleaned by rinsing and infiltration of water, acetone and ethanol, in sequence, in order to remove acid residue. Free-standing coatings were heated at 1315 °C at heating rate of 6 °C/min in an air furnace and hold at the highest temperature for 2, 10 and 50 h, respectively. Then they were slowly furnace cooled down to room temperature. The specimens were studied in free-standing state because the temperature chosen for the tests was above the capability of the metal substrate.

2.2. Phase analysis

Phase composition of as-sprayed and annealed YSZ coatings was investigated by using an X-ray Powder Diffractometer (PW1880, Philips, Almelo, The Netherlands) operating with Cu Kα radiation produced at 40 kV and 40 mA. The 2θ scan was performed between 20° and 90° by step width of 0.02°. The time per step was set to 5 s.

The Rietveld refinement was employed for quantitative analysis of XRD patterns of as-sprayed and annealed YSZ coatings, by using the free software Maud (Material Analysis Using Diffraction, version 2.074, Luca Lutterotti, University of Trento, Italy) and following the same procedure described in a previous work [19]. Rietveld quantitative analysis has to be carefully performed due to the coexistence of several zirconia phases, whose peaks are partially overlapped. Thereby, it was performed in well-determined ranges of the diffraction patterns, in order to guarantee the accuracy of the measurements. The low-angle region (27–32°) was considered to calculate the amount of the monoclinic phase, while the high-angle region (72–75°) was considered to calculate the relative proportions of tetragonal t', tetragonal t and cubic c zirconia phases. Indeed, a part from the monoclinic phase three other zirconia phases could be detected: a high-yttria tetragonal t' phase, a low-yttria tetragonal t phase and a high-yttria cubic c phase. Their lattice parameters depend on the yttria content. The t' phase can be distinguished from the t phase by means of its smaller c/a lattice parameter ratio, *i.e.* higher stabilizer content.

The yttria content in both tetragonal zirconia phases was quantified by using the formula reported by Ilavsky and Stalick [15]:

$$Y_2O_3\,(\text{mol.}\%) = \frac{(1.0225 - c/a\sqrt{2})}{0.0016}$$

where a [Å] and c [Å] are the lattice parameters for each tetragonal phase.

In turn, the yttria content of the cubic phase was calculated from the equation [14]:

$$Y_2O_3\,(\text{mol.}\%) = \frac{(a - 5.1159)}{0.001647}$$

where a [Å] is the lattice parameter of the cubic phase.

2.3. Thermophysical properties

For thermal expansion and specific heat capacity measurements free-standing YSZ coatings were cut to desired dimensions. In particular, the linear thermal expansion of as-sprayed and annealed YSZ coatings was measured using a Netzsch dilatometer (TMA 402, Netzsch-Geratebäu GmbH, Selb, Germany) in static air atmosphere. The model herein employed is a vertically quartz pushrod type using a linear variable displacement transducer (LVDT) with thermo-stated housing. The thermal expansion measurements were carried out on free-standing coatings (sample length = 7 mm), from room temperature up to 900 °C at heating rate of 10 °C/min. Three consecutive scans were collected for each type of samples and both in-plane and out-of-plane thermal expansions were measured. To check the accuracy of the pushrod dilatometer three measurements in the same conditions were performed on a synthetic sapphire (NS SRM 732) from room temperature to 900 °C. The measured mean CTE was compared with the mean value of the standard material reported in the literature ($9.2 \times 10^{-6}\,K^{-1}$). The accuracy was of about 3%.

Specific heat measurements were performed between room temperature and 1250 °C using a simultaneous thermal analyzer (Model STA 429, Netzsch-Geratebäu GmbH, Selb, Germany) equipped with a sample holder for differential scanning calorimetry (DSC). The measurements were carried out in static air at 10 °C/min on approximately 3 mm × 3 mm × 2 mm sized samples. The sample weight used for C_p measurement was approximately 120 mg. Three consecutive measurement cycles were considered for heat capacity calculation. The ratio method using a synthetic sapphire as calibrant was used to determine the specific heat curves of YSZ coatings [19,20].

3. Results and discussion

3.1. Phase analysis

The whole XRD patterns of YSZ feedstock, as-sprayed and annealed coatings are reported in Fig. 1. The as-sprayed coatings are mainly composed of tetragonal t' zirconia phase,

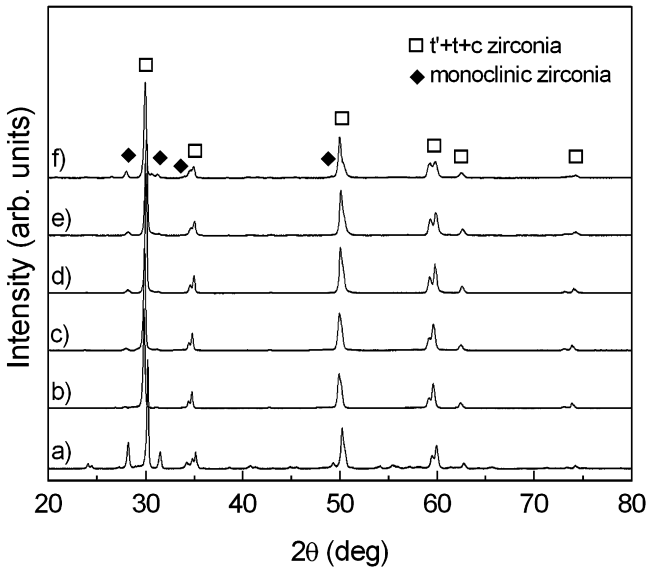

Fig. 1. XRD patterns of YSZ feedstock and coatings: (a) feedstock; (b) as-sprayed – rapidly cooled; (c) as-sprayed – slowly cooled; (d) annealed for 2 h; (e) annealed for 10 h; (f) annealed for 50 h.

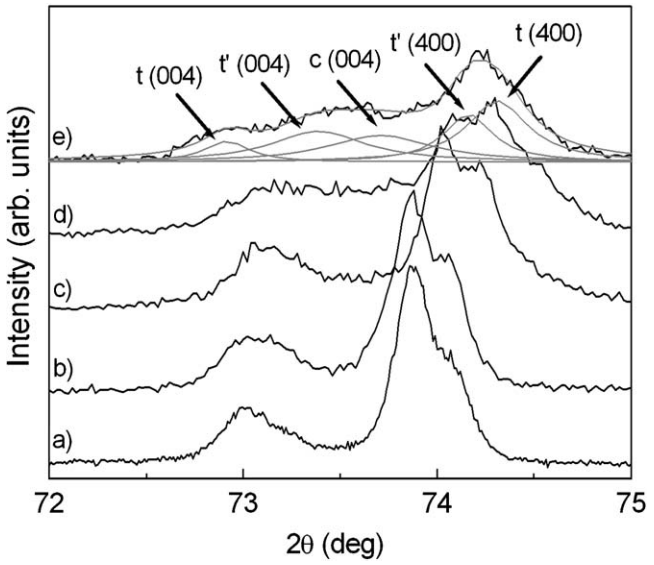

Fig. 3. High-angle range of the diffraction patterns for YSZ coatings: (a) as-sprayed – rapidly cooled; (b) as-sprayed – slowly cooled; (c) annealed for 2 h; (d) annealed for 10 h; (e) annealed for 50 h.

with smaller amounts of stable tetragonal *t*, cubic *c* and monoclinic *m* zirconia phases, according to JCPDS (No. 81-1544 for tetragonal, No. 49-1642 for cubic and No. 37-1484 for monoclinic zirconia) available at the International Centre for Diffraction Data (ICDD). Shift in peak positions can be related to microstrains and different yttria contents in each zirconia phase, as discussed later.

Figs. 2 and 3 show low-angle (27–32°) and high-angle (72–75°) regions of XRD patterns, respectively. Fig. 2 shows the (1 1 1) peak for ($t' + t + c$) zirconia and the (1 1 $\underline{1}$) and (1 1 1) peaks for monoclinic zirconia. In Fig. 3 the (0 0 4) and (4 0 0) peaks for both t' and *t* zirconia phases are detectable, as well as the (0 0 4) peak for the cubic phase. A qualitative example of peak deconvolution is illustrated for YSZ coating aged for 50 h.

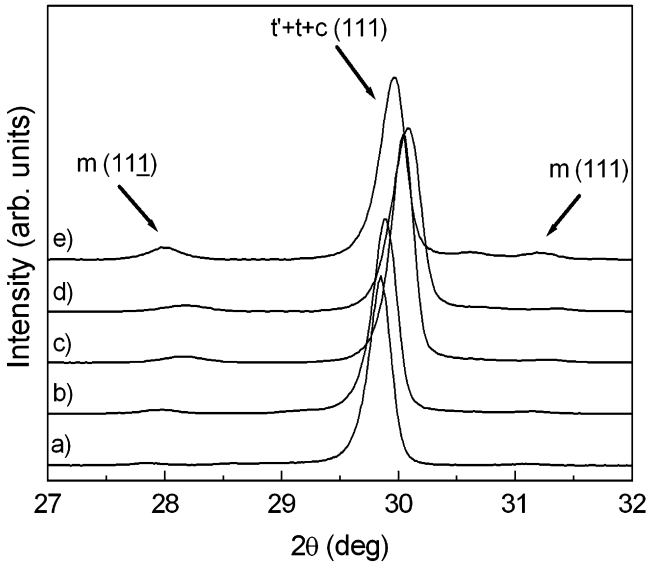

Fig. 2. Low-angle range of the diffraction patterns for YSZ coatings: (a) as-sprayed – rapidly cooled; (b) as-sprayed – slowly cooled; (c) annealed for 2 h; (d) annealed for 10 h; (e) annealed for 50 h.

Different cooling rates employed during plasma spraying or thermal treatment of YSZ coatings can promote remarkable chemical and physical reactions, such as reduction to lower valence states, stabilizing oxide depletion or enrichment, formation of zirconium and yttrium sub-oxides and impurity segregation phenomena [21].

More precisely, when the samples are forced air cooled during deposition the molten splats are rapidly quenched and, therefore, the high oxygen vacancies formed at high-temperature tend to be retained at room temperature, suppressing the tetragonal-to-monoclinic transformation. The coating is mainly composed of metastable tetragonal t' phase (∼92.9%), with small traces of cubic c and monoclinic m phases, while stable tetragonal *t* phase is absent.

Otherwise, a slow cooling rate reduces the level of oxygen vacancies and can promote the transformation of the tetragonal phase to the monoclinic phase, promoting possible compressive stresses in as-produced coatings. However, in our experiments the content of monoclinic phase found in slowly cooled coatings is slightly higher than that found in rapidly cooled ones, *i.e.* 4.2% and 5%, respectively. Therefore, it can be supposed that the monoclinic phase is substantially associated to unmelted or partially melted particles embedded in coating microstructure. To this purpose, it should be noted that the feedstock herein employed is characterized by a large amount of monoclinic phase (m = 36.8% and t' = 63.2%). Moreover, slowly cooled coatings contain a little amount of stable tetragonal phase, equal to 1.9%.

As shown in Table 3, the content of the monoclinic phase tends to gradually increase with increasing the aging time up to 13.8% after 50 h. The peaks for monoclinic zirconia are rather broad, suggesting a very low grain size, and then their width slightly decreases with increasing the aging time. The presence of relatively large amount of monoclinic phase at room

Table 3
Relative percentages, lattice parameters and yttria contents for zirconia phases in as-sprayed and annealed YSZ coatings (Rietveld analysis).

Sample	*c*-ZrO_2 (%)	*c* [Å]	Yttria content (%)	*t'*-ZrO_2 (%)	*a* [Å]	*c* [Å]	Yttria content (%)	*t*-ZrO_2 (%)	*a* [Å]	*c* [Å]	Yttria content (%)	*m*-ZrO_2 (%)	RP
Feedstock	–	–	–	63.2	3.6126	5.1600	7.82	–	–	–	–	36.8	10.3
As-sprayed (rapidly cooled)	2.9	5.1450	18.81	92.9	3.6251	5.1810	7.44	–	–	–	–	4.2	11.8
As-sprayed (slowly cooled)	3.5	5.1430	17.52	89.6	3.6259	5.1785	7.89	1.9	3.6162	5.1922	4.52	5.0	10.6
Annealed 1315 °C, 2 h	6.2	5.1393	15.13	70.4	3.6193	5.1747	7.20	15.8	3.6078	5.1882	3.53	7.6	10.9
Annealed 1315 °C, 10 h	13.5	5.1388	14.80	43.4	3.6168	5.1702	7.31	33.2	3.6045	5.1857	3.25	9.9	10.7
Annealed, 1315 °C, 50 h	16.1	5.1405	15.90	35.5	3.6178	5.1682	7.73	34.6	3.6078	5.1902	3.28	13.8	10.8

temperature has been also noticed in YSZ coatings annealed or thermally shocked at 1300 °C (up to 20%) [22,23]. It should be noted that the shape of the peak at ~30° depends on the relative proportions of cubic and tetragonal phases and the corresponding grain size.

To calculate their relative proportions, the high-angle (72–75°) range has to be considered. As shown in Fig. 3, the metastable t' phase is unstable during high-temperature exposure and decomposes into low-yttria tetragonal phase and high-yttria cubic phase, due to the gradual diffusion of yttria stabilizer. In particular, the excess of yttria allows the nucleation and growth of cubic zirconia grains. The peak intensities for stable tetragonal *t* and cubic *c* phases increase with increasing the aging time, as well as their amounts, while the content of metastable t' decreases. During slow cooling to room temperature the cubic phase may be retained or may transform to tetragonal phase, whereas low-yttria tetragonal phase may transform to monoclinic, depending on the grain growth. The transformation of tetragonal to monoclinic zirconia is noticed prior to the full decomposition of t' phase. Therefore, t', *t*, *c* and *m* zirconia phases coexist in annealed YSZ coatings. The small grain size of the *t* phase (the corresponding peaks are broader than those corresponding to the t′ phase) and the retained amount of yttria in the same phase reduce the extent of the monoclinic transformation.

The calculated percentages of zirconia phases, as well as their unit cell dimensions and the corresponding contents of yttria stabilizer are summarized in Table 3. The R_p parameters, representative of the quality of the fit, are also reported. After 50 h of heat treatment, a significant amount of the metastable t' phase (35.5%) is still present, together to the cubic c phase and the stable tetragonal *t* phases (16.1% and 34.6%, respectively). Therefore, long-term exposures are needed to promote the total decomposition of t' phase. It should be noted that the lattice constants increase with increasing the yttria content. The yttria content in the cubic phase is higher in as-sprayed coatings. With increasing the aging time, it firstly decreases and then increases up to 15.9%. The yttria content in t' phase is in the range from 7.2% to 7.9%, while the yttria content in *t* phase is between 3.2% and 4.5%. The rapid diffusion of yttria generates lower and high-yttria regions, so that no zirconia phases with intermediate stabilizer contents are observed. The phase stability can be affected by spraying parameters, as well as by microstructural features, which can locally change due to yttria fluctuations from grain to grain.

It is worth noting that high-temperature phase evolution of plasma sprayed YSZ coatings is substantially different from that found for ceria–yttria co-stabilized zirconia (CYSZ) coatings and, therefore, strongly depends on the nature and the amount of the oxides used as zirconia stabilizers [19].

3.2. Thermal expansion

Thermal expansion curves of as-sprayed and annealed YSZ coatings are plotted in Figs. 4 and 5. Fig. 4 shows in-plane thermal expansion of as-sprayed and annealed YSZ samples between 50 °C and 900 °C. It can clearly be seen that thermal

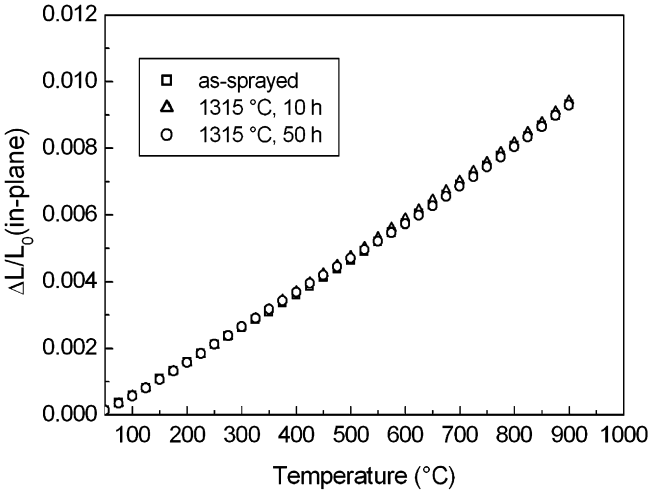

Fig. 4. In-plane thermal expansion curves for as-sprayed and annealed YSZ coatings.

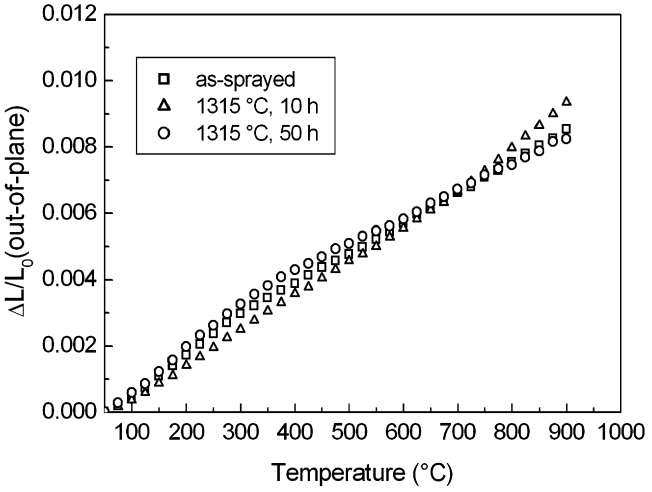

Fig. 5. Out-of-plane thermal expansion curves for as-sprayed and annealed YSZ coatings.

expansion increases linearly over the entire temperature range and the shrinkage for as-sprayed and annealed YSZ coatings is approximately 0.93–0.94%.

The out-of-plane thermal expansion curves of as-sprayed and annealed YSZ coatings are shown in Fig. 5. The values of the shrinkage are influenced by the annealing time and are in the range between 0.82% and 0.94%. YSZ coatings annealed for 10 h show the highest thermal expansion, while the corresponding values for as-sprayed and 50 h annealed coatings are ~13% smaller. Therefore, we can deduce that high-temperature sintering of the porous microstructure is more sensitive to the formation of sintering necks at splat boundaries rather than to the closure of intralamellar microcracks which are of lower size, as also observed for plasma sprayed CYSZ coatings [1,24].

The mean values of thermal expansion coefficients for as-sprayed and heat-treated YSZ coatings are given in Table 4. The in-plane CTE is approximately $10.7 \times 10^{-6}\,K^{-1}$ for as-sprayed and annealed YSZ coatings between 50 °C and 900 °C. This

Table 4
In-plane (αx) and out-of-plane (αZ) thermal expansion coefficients for as-sprayed and annealed YSZ coatings.

Coating	α_x (50–900 °C) [$10^{-6}\,K^{-1}$]	α_Z (50–300 °C) [$10^{-6}\,K^{-1}$]	α_Z (300–900 °C) [$10^{-6}\,K^{-1}$]
As-sprayed	10.73	12.33	9.17
Annealed 1315 °C, 10 h	10.94	10.25	11.13
Annealed 1315 °C, 50 h	10.67	13.42	8.16

value is higher than those reported in any previous works [17,25] and more close to the results found by Schwingel et al. for plasma sprayed YSZ coatings [26]. On the contrary, the out-of-plane CTE is more sensitive to the thermal aging. A single linear fit of the experimental points between 50 °C and 900 °C provides CTE values in the range between $9.49 \times 10^{-6}\,K^{-1}$ and $10.82 \times 10^{-6}\,K^{-1}$ (the lowest value is found for the coating aged for 50 h). However, if we carefully observe the thermal expansion curves, we can see that at temperatures higher than 300 °C a change in their slope can be noticed and a corresponding decrease of the thermal expansion coefficient, except for YSZ coatings treated for 10 h. Taking into consideration this behaviour, CTE values vary from $10.3 \times 10^{-6}\,K^{-1}$ to $13.4 \times 10^{-6}\,K^{-1}$ between 50 °C and 300 °C and from $8.2 \times 10^{-6}\,K^{-1}$ to $11.1 \times 10^{-6}\,K^{-1}$ between 300 °C and 900 °C.

To this purpose, it should be noted that the CTE is strongly related to the crystal structure of the coating and to any phase transitions which could occur during heating. Indeed, at about 300 °C part of the tetragonal phase may transform to monoclinic, while at temperature higher than 600 °C the monoclinic phase may transform to the tetragonal one. These transformations have been noticed for annealed or thermally shocked YSZ coatings [13,23]. Moreover, the microstructural properties can locally vary within each coating, as well as the concentration of yttria from grain to grain or within a grain. In addition, the shrinkage and the sintering characteristics can be strongly influenced by the presence of relatively small impurities within the coating. These impurities can enhance the diffusion rates for grain boundaries, lattice and surface diffusion [27,28]. In particular, the possible formation of a glassy phase at grain boundaries plays a significant role on the grain growth and, therefore, on the sintering rate [21]. All these aspects may be responsible for the fluctuations in CTE values. Otherwise, we can surely argue that no sintering occurs during measurements up to 900 °C.

In-plane CTE of YSZ coatings is lower than that of CYSZ ones (~$12.6 \times 10^{-6}\,K^{-1}$ for as-produced CYSZ coating), due to the different amount of oxygen vacancies. The CTE generally increases with increasing the oxygen vacancies, even if Hayashi et al. have reported that it decreases with increasing the yttria content for sintered YSZ samples [29].

To the purpose, it is worth noting that, when a ceramic TBC is applied on a metal substrate, the thermal expansion mismatch can promote tensile stresses and then the formation and the propagation of cracks within the same TBC, reducing the sintering effect.

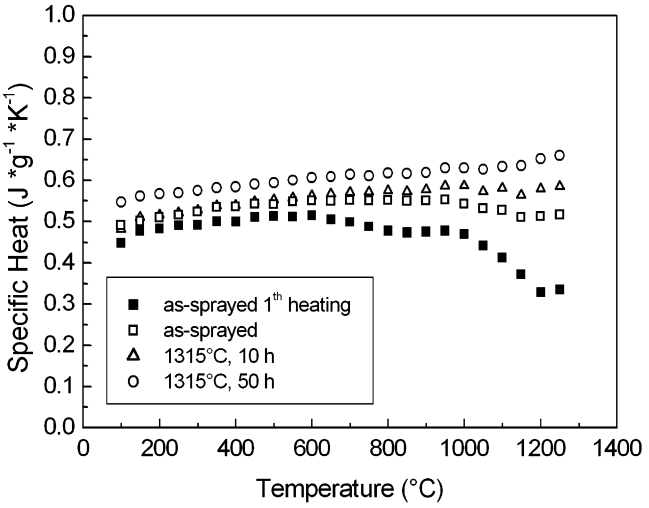

Fig. 6. Specific heat capacity of as-sprayed and annealed YSZ coatings as a function of temperature.

3.3. Heat capacity

In Fig. 6 the specific heat curves of as-sprayed and thermally aged YSZ coatings are plotted as a function of temperature. $C_p(T)$ curves were calculated as a mean value of three consecutive measurement cycles. For as-produced coatings two different curves are reported. The former corresponds to the first heating cycle, while the latter is the average of three successive measurement cycles. Indeed, it is worth noting that the first heating provides some irreversible changes, such as first-stage sintering and stress relaxation, and a corresponding increase of heat capacity at high temperature, whereas no deviations were observed in the next runs. Changes at crystal lattice scale may also have a significant effect on C_p values, since during heating a decrease of structural defects can occur.

The specific heat increases gradually as the temperature increases. For as-sprayed YSZ coating C_p value is found to be 0.49 J K^{-1} g^{-1} at 100 °C and 0.52 J K^{-1} g^{-1} at 1250 °C. These values are lower than those reported by other authors for YSZ sintered samples and plasma sprayed coatings [30,31]. For coatings exposed for 50 h C_p value is found to be 0.55 J K^{-1} g^{-1} at 100 °C and 0.66 J K^{-1} g^{-1} at 1250 °C.

Therefore, the specific heat capacity increases with increasing the aging time, due to high-temperature sintering of the porous microstructure, grain growth and decomposition of the metastable t' phase. The healing of vertical microcracks as well as an enhanced bonding at splat boundaries promoted by grain growth and microcracks closure produce a partial densification of the porous microstructure, reducing the porosity volume and correspondingly increasing the elastic modulus [8,24,28]. Therefore, the TBC becomes less strain tolerant and more heat conductive. As a consequence, the thermal insulation could be notably reduced after long-term high-temperature exposure, even if the main changes typically occur after relatively short times and then the sintering activity tends to stabilize. However, sintering can also affect the shape and the size of globular pores to a lesser extent, as well as the formation of equiaxed grains [19,24].

In conclusion, thermal annealing of YSZ coatings produces an increase of specific heat capacity, while a slight decrease has been observed for CYSZ coatings treated at the same conditions. The different evolution of thermophysical properties of these zirconia-based TBC systems can be explained in terms of different phase compositions and sintering behaviour.

4. Conclusions

Yttria partially stabilized zirconia coatings were deposited by Atmospheric Plasma Spraying and annealed at 1315 °C for different durations. The cooling rate during deposition slightly influenced the retention of tetragonal t' and monoclinic phases at room temperature. Indeed, the monoclinic phase was substantially associated to the presence of unmelted or partially melted particles. High-temperature exposure produced the partial decomposition of tetragonal t' phase and the corresponding increase in the content of stable tetragonal, cubic and monoclinic zirconia phases.

The thermal expansion coefficient was equal to 10.7×10^{-6} K^{-1} in plane direction and kept almost constant after isothermal annealing. On the other hand, CTE changed in through-thickness direction with increasing the aging time. In particular, during the heating cycle some changes in the slope of thermal expansion curves were noticed, probably to any phase transitions between tetragonal and monoclinic phases, to local fluctuations in the yttria content and to the presence of retained impurities in YSZ coatings.

The specific heat capacity increased with increasing the aging time due to high-temperature sintering of the porous microstructure.

The future researches will be devoted to the study of alternative TBC systems and great attention will be focused on plasma sprayed nanostructured coatings.

References

[1] M. Alfano, G. Di Girolamo, L. Pagnotta, D. Sun, Processing, microstructure and mechanical properties of air plasma-sprayed ceria–yttria co-stabilized zirconia coatings, Strain (2010), doi:10.1111/j.1475-1305.2009.00659.x.
[2] T.M. Yonushonis, Overview of thermal barrier coatings in diesel engines, J. Therm. Spray Technol. 6 (1) (1997) 50–56.
[3] H.B. Guo, R. Vassen, D. Stöver, Thermophysical properties and thermal cycling behavior of plasma sprayed thick thermal barrier coatings, Surf. Coat. Technol. 192 (2005) 48–56.
[4] R. Vassen, G. Kerkhoff, D. Stöver, Development of a micromechanical life prediction model for plasma sprayed thermal barrier coatings, Mater. Sci. Eng. A303 (2001) 100–109.
[5] D. Stöver, G. Pratch, H. Lehmann, M. Dietrich, J.E. Döring, R. Vassen, New material concept for the next generation of plasma-sprayed thermal barrier coatings, J. Therm. Spray Technol. 13 (1) (2003) 76–83.
[6] M.O. Jarligo, D.E. Mack, R. Vassen, D. Stöver, Plasma-sprayed complex perovskites as thermal barrier coatings, J. Therm. Spray Technol. 18 (2) (2009) 187–193.
[7] C.G. Levi, Emerging materials and processes for thermal barrier systems, Curr. Opin. Solid State Mater. Res. 33 (2004) 383–417.

[8] S. Paul, A. Cipitria, S.A. Tsipas, T.W. Clyne, Sintering characteristics of plasma sprayed zirconia containing different stabilizers, Surf. Coat. Technol. 203 (2009) 1069–1074.
[9] R. Vassen, A. Stuke, D. Stöver, Recents developments in the field of thermal barrier coatings, J. Therm. Spray Technol. 18 (2) (2009) 181–186.
[10] Y. Tan, J.P. Longtin, S. Sampath, H. Wang, The effect of the starting microstructure on the thermal properties of as-sprayed and thermally exposed plasma-sprayed YSZ coatings, J. Am. Ceram. Soc. 92 (3) (2009) 710–716.
[11] G. Mauer, D. Sebold, R. Vassen, D. Stöver, Characterization of plasma-sprayed yttria-stabilized zirconia coatings by cathodoluminescence, J. Therm. Spray Technol. 18 (4) (2009) 572–577.
[12] G. Witz, V. Shklover, W. Steurer, S. Bachegowda, H.P. Bossmann, Phase evolution in yttria-stabilized zirconia thermal barrier coatings studied by Rietveld refinement of X-ray powder diffraction patterns, J. Am. Ceram. Soc. 90 (9) (2007) 2935–2940.
[13] J.R. Brandon, R. Taylor, Phase stability of zirconia-based thermal barrier coatings. Part I. Zirconia-yttria alloys, Surf. Coat. Technol. 46 (1991) 75–90.
[14] J. Ilavsky, J.K. Stalick, J. Wallace, Thermal spray yttria-stabilized zirconia phase changes during annealing, J. Therm. Spray Technol. 10 (3) (2001) 497–501.
[15] J. Ilavsky, J.K. Stalick, Phase composition and its changes during annealing of plasma-sprayed YSZ, Surf. Coat. Technol. 127 (2–3) (2000) 120–129.
[16] J. Moon, H. Choi, H. Kim, C. Lee, The effects of heat treatment on the phase transformation behavior of plasma-sprayed stabilized ZrO_2 coatings, Surf. Coat. Technol. 155 (2002) 1–10.
[17] S. Ahmaniemi, P. Vuoristo, T. Mantyla, F. Cernuschi, L. Lorenzoni, Modified thick thermal barrier coatings: thermophysical characterization, J. Eur. Ceram. Soc. 24 (2004) 2669–2679.
[18] R.A. Miller, J.L. Smialek, R.G. Garlick, Phase stability in plasma-sprayed partially stabilized zirconia-yttria, in: A.H. Heuer, L.W. Hobbs (Eds.), Advances in Ceramics, Science and Technology of Zirconia, vol. 3, American Ceramic Society, Columbus, OH, 1991, pp. 241–251.
[19] G. Di Girolamo, C. Blasi, M. Schioppa, L. Tapfer, Structure and thermal properties of heat treated plasma sprayed ceria–yttria co-stabilized zirconia coatings, Ceram. Int. 36 (2010) 961–968.
[20] J.B. Henderson, W.D. Emmerich, E. Wassmer, Measurement of the specific heat and heat of decomposition of a polymer composite to high temperatures, J. Therm. Anal. 33 (4) (1988) 1067–1077.
[21] G.M. Ingo, T. De Caro, Chemical aspects of plasma spraying of zirconia-based thermal barrier coatings, Acta Mater. 56 (2008) 5177–5187.
[22] U. Schulz, Phase transformation in EB-PVD yttria partially stabilized zirconia thermal barrier coatings during annealing, J. Am. Ceram. Soc. 83 (4) (2000) 904–910.
[23] C.H. Lee, H.K. Kim, H.S. Choi, H.S. Ahn, Phase transformation and bond coat oxidation behavior of plasma-sprayed zirconia thermal barrier coatings, Surf. Coat. Technol. 124 (2000) 1–12.
[24] M. Alfano, G. Di Girolamo, L. Pagnotta, D. Sun, J. Zekonyte, R.J. Wood, The influence of high temperature sintering on microstructure and mechanical properties of APS CeO_2–Y_2O_3–ZrO_2 coatings, J. Mater. Sci. 45 (2010) 2662–2669.
[25] W. Ma, D.E. Mack, R. Vassen, D. Stöver, Perovskite-type strontium zirconate as a new material for thermal barrier coatings, J. Am. Ceram. Soc. 91 (8) (2008) 2630–2635.
[26] D. Schwingel, R. Taylor, T. Haubold, J. Wigren, C. Gualco, Mechanical and thermophysical properties of thick PYSZ thermal barrier coatings: correlation with microstructure and spraying parameters, Surf. Coat. Technol. 108–109 (1998) 99–106.
[27] R. Vassen, N. Czech, W. Malléner, W. Stamm, D. Stöver, Influence of impurity content and porosity of plasma-sprayed yttria-stabilized zirconia layers on the sintering behaviour, Surf. Coat. Technol. 141 (2001) 135–140.
[28] S. Paul, A. Cipitria, I.O. Golosnoy, L. Xie, M.R. Dorfman, T.W. Clyne, Effects of impurity content on the sintering characteristics of plasma-sprayed zirconia, J. Therm. Spray Technol. 16 (5–6) (2007) 798–803.
[29] H. Hayashi, T. Saitou, N. Maruyama, H. Inaba, K. Kawamura, M. Mori, Thermal expansion coefficient of yttria stabilized zirconia for various yttria contents, Solid State Ionics 176 (2005) 613–619.
[30] R. Vassen, X. Cao, F. Tietz, D. Basu, D. Stöver, Zirconates as new materials for thermal barrier coatings, J. Am. Ceram. Soc. 83 (8) (2000) 2023–2028.
[31] F. Cernuschi, L. Lorenzoni, S. Ahmaniemi, P. Vuoristo, T. Mantyla, Studies of the sintering kinetics of thick thermal barrier coatings by thermal diffusivity measurements, J. Eur. Ceram. Soc. 25 (2005) 393–400.